LBL-17948

Lawrence Berkeley Laboratory
UNIVERSITY OF CALIFORNIA

RECEIVED
LAWRENCE
BERKELEY LABORATORY

AUG 20 1984

LIBRARY AND
DOCUMENTS SECTION

To be published as a chapter in Biological Effects and Dosimetry of Non-Ionizing Radiation: Static and ELF Electromagnetic Fields, M. Grandolfo, S.M. Michaelson, and A. Rindi, Eds., Plenum Press, New York, 1984

MECHANISMS FOR BIOLOGICAL EFFECTS OF MAGNETIC FIELDS

T.S. Tenforde

May 1984

TWO-WEEK LOAN COPY

This is a Library Circulating Copy which may be borrowed for two weeks.

Donner Laboratory

Biology & Medicine Division

Prepared for the U.S. Department of Energy under Contract DE-AC03-76SF00098

LBL-17948

DISCLAIMER

This document was prepared as an account of work sponsored by the United States Government. While this document is believed to contain correct information, neither the United States Government nor any agency thereof, nor the Regents of the University of California, nor any of their employees, makes any warranty, express or implied, or assumes any legal responsibility for the accuracy, completeness, or usefulness of any information, apparatus, product, or process disclosed, or represents that its use would not infringe privately owned rights. Reference herein to any specific commercial product, process, or service by its trade name, trademark, manufacturer, or otherwise, does not necessarily constitute or imply its endorsement, recommendation, or favoring by the United States Government or any agency thereof, or the Regents of the University of California. The views and opinions of authors expressed herein do not necessarily state or reflect those of the United States Government or any agency thereof or the Regents of the University of California.

LBL-17948

MECHANISMS FOR BIOLOGICAL EFFECTS OF MAGNETIC FIELDS

T.S. Tenforde

Biology and Medicine Division

Lawrence Berkeley Laboratory

University of California

Berkeley, California 94720

May, 1984

CHAPTER SUBMITTED FOR PUBLICATION IN:

BIOLOGICAL EFFECTS AND DOSIMETRY OF NON-IONIZING RADIATION: STATIC AND ELF ELECTROMAGNETIC FIELDS. M. GRANDOLFO, S.M. MICHAELSON, AND A. RINDI, EDS. PLENUM PRESS, NEW YORK. IN PRESS, 1984.

This work was supported by the U.S. Department of Energy under Contract DE-AC03-76SF00098.

MECHANISMS FOR BIOLOGICAL EFFECTS OF MAGNETIC FIELDS

T.S. Tenforde

Biology and Medicine Division
Lawrence Berkeley Laboratory
University of California
Berkeley, California 94720

CONTENTS:

INTRODUCTION

QUANTITIES AND UNITS

STATIONARY MAGNETIC FIELDS

Electrodynamic and Magnetohydrodynamic Interactions

Magnetomechanical Effects:

1. Orientation of Diamagnetically Anisotropic Macromolecules
2. Orientation of Organisms with Permanent Magnetic Moments
3. Translation of Paramagnetic Substances in a Magnetic Field Gradient

Magnetic Field Interactions at the Atomic and Nuclear Levels:

1. Nuclear Magnetic Resonance
2. Charge Transfer Reactions

TIME-VARYING MAGNETIC FIELDS

MECHANISMS FOR BIOLOGICAL EFFECTS OF MAGNETIC FIELDS

T. S. Tenforde

Biology and Medicine Division
Lawrence Berkeley Laboratory
University of California
Berkeley, California

INTRODUCTION

One of the most interesting and challenging aspects of research on the biological effects of magnetic fields is the broad spectrum of potential interaction mechanisms between these fields and living tissues. At the level of macromolecules and larger structures, interactions of stationary magnetic fields with biological systems can be characterized as electrodynamic or magnetomechanical in nature. Electrodynamic effects originate through the interaction of magnetic fields with electrolyte flows, leading to the induction of electrical potentials and currents. Magnetomechanical phenomena include orientation of magnetically anisotropic macromolecules in strong homogenous fields, and the translation of paramagnetic species in strong gradient fields. Magnetic fields that are time-varying also interact with living tissues at the macroscopic and microscopic levels to produce circulating currents via the mechanism of magnetic induction. Each of these interaction mechanisms will be described from a theoretical viewpoint in this chapter, and their applicability to biologically relevant systems will be illustrated with selected examples.

At the atomic and subatomic levels, several types of magnetic field interactions have been demonstrated to occur in biological systems. In this chapter two such interactions will be described, namely, the use of nuclear magnetic resonance for imaging proton density in living tissues and the influence of Zeeman interactions on certain classes of electron transfer reactions. Several speculative theories of magnetic field interactions at the atomic and molecular levels, such as the potential role of superconducting

junctions in biological materials,[1-7] will not be discussed.

QUANTITIES AND UNITS

The fundamental vector quantities describing a magnetic field are $\vec{H}$, the intensity, and $\vec{B}$, the magnetic flux density (or equivalently, the magnetic induction). The field intensity can be calculated from the circuital form of Ampere's law:

$$\oint \vec{H} \cdot d\vec{\ell} = I \tag{1}$$

where $d\vec{\ell}$ is a vector element of length along a closed path that bounds an area through which a net current, I, flows. The MKS and CGS units of $\vec{H}$ are, respectively, A/m and Oersted (or Gauss). The conversion factor relating the MKS and CGS units for $\vec{H}$ is $1\ A/m = (4\pi/10^3)$ Oersted.

The magnetic flux density is defined in terms of the force $\vec{F}$ exerted on a charge q moving with a velocity $\vec{v}$:

$$\vec{F} = q\ [\vec{v} \times \vec{B}] \tag{2}$$

where the term in brackets is the cross product of the vectors $\vec{v}$ and $\vec{B}$. The MKS and CGS units of $\vec{B}$ are N/A•m (= Tesla) and Gauss, respectively. The conversion factor between the MKS and CGS units for $\vec{B}$ is 1 Tesla = 10^4 Gauss.

The relationship between the quantities $\vec{H}$ and $\vec{B}$ is given by the equation:

$$\vec{B} = \mu_0(\vec{H} + \vec{M}) \tag{3}$$

where μ_0 = permeability of free space and $\vec{M}$ = magnetization per unit volume. The units of $\vec{H}$ and $\vec{M}$ are identical regardless of which system of units is used. In the CGS system μ_0 is a dimensionless quantity equal to unity, and in the MKS system $\mu_0 = 4\pi \times 10^{-7}\ N/A^2$. In an isotropic medium $\vec{M}$ and $\vec{H}$ are linearly related by the scalar magnetic susceptibility χ:

$$\vec{M} = \chi\vec{H} \tag{4}$$

For diamagnetic substances $\chi < 0$, and for paramagnetic and ferromagnetic materials $\chi > 0$. Using eqn. (4), the relation between $\vec{H}$ and $\vec{B}$ given by eqn. (3) becomes:

$$\vec{B} = \mu_0(1 + \chi)\vec{H} = \mu\vec{H} \tag{5}$$

where μ is the magnetic permeability of the medium. It is often convenient to discuss magnetic materials in terms of the relative permeability μ_r, which is a dimensionless parameter defined by the relation:

$$\mu_r = \mu/\mu_0 = 1 + \chi \tag{6}$$

The value of μ_r is therefore a measure of the magnetic permeability of a medium relative to free space.

Most biological materials are very weakly diamagnetic, and $\mu_r \simeq 1$. As a result, $\vec{B} \simeq \mu_0 \vec{H}$ and in the CGS system of units $\vec{B}$ can be set equal to $\vec{H}$ as a close approximation. This convention has been used extensively in the biological literature, where many authors have used $\vec{B}$ and $\vec{H}$ as interchangeable quantities. Many biological publications therefore contain equations that are appropriate for use only with the CGS system of units since the permeability of free space, μ_0, has been omitted. In the remainder of this chapter, all of the fundamental equations will be presented in a general form in which $\vec{H}$ and $\vec{B}$ are maintained as separate field quantities.

STATIONARY MAGNETIC FIELDS

Electrodynamic and Magnetohydrodynamic Interactions

Steady flows of ionic currents interact with applied stationary magnetic fields via the well known Lorentz force law:

$$\vec{F} = q\,[\vec{E} + \vec{v} \times \vec{B}] \tag{7}$$

where $\vec{F}$ is the net force exerted on a charge q moving with velocity $\vec{v}$, $\vec{E}$ is the local electric field intensity, and $\vec{B}$ is the magnetic flux density. In the case of electrolyte flows through electrically insulated channels (e.g., blood vessels), the interaction of an applied magnetic field with the ionic charge carriers under steady-state conditions will induce a local electric field of magnitude $\vec{E} = -\vec{v} \times \vec{B}$. The induced field, $\vec{E}$, is transverse to both $\vec{v}$ and $\vec{B}$. This phenomenon, which is the basis of the Hall effect in solid state materials, is also relevant to biological processes that involve electrolytic conduction.

An interesting example of the role of magnetically-induced electrical potentials in a biological system is the geomagnetic direction-finding mechanism used by elasmobranch fishes, which include sharks, skates and rays.[8-10] The heads of these animals contain long jelly-filled canals known as the ampullae of Lorenzini, which have a high electrical conductivity similar to

that of seawater. As the fish swims through the earth's magnetic field, a small voltage gradient is induced in the canals which is detected by the sensory epithelia lining the terminal ampullary region. The induced field, which can be detected at levels as low as 0.5 μV/m,[11] has a distinct polarity that is dependent upon the relative orientation of the geomagnetic field and the direction of swimming. In this way, the marine elasmobranchs use the $-\vec{v} \times \vec{B}$ fields induced in their ampullary canals as a directional compass.

A second example of induced electrical potentials is provided by blood flow in the presence of an applied stationary magnetic field. For the specific case of a cylindrical vessel with a diameter d, the magnitude of the induced potential, ψ, is given by:

$$\psi = |\vec{E}|\, d = |\vec{v}||\vec{B}| d \sin \theta \qquad (8)$$

where θ is the angle between the mean axial flow velocity, $\vec{v}$, and $\vec{B}$. This relationship, which was originally derived by Kolin in a rigorous theoretical treatment,[12] is the physical basis of the electromagnetic flowmeter.[13,14] From eqn. (8) it can be predicted that ψ varies linearly with the vessel diameter and the magnetic field strength, and is strongly dependent upon the orientation of the flow relative to the external field. A maximum value of ψ is obtained when the blood flow direction and the applied field are orthogonal.

The existence of magnetically-induced blood flow potentials in the central circulatory systems of several species of mammals has been demonstrated experimentally.[15-19] These induced potentials can be conveniently studied from electrocardiogram (ECG) records obtained with surface electrodes, as demonstrated in Fig. 1 for a rat exposed to stationary magnetic fields up to 2.10 T. The ECG signal in the T-wave region shows a substantial augmentation in the presence of fields greater than 0.3 T, and this phenomenon is completely and immediately reversible upon termination of the magnetic field exposure. Based upon its temporal sequence in the ECG record, the increased amplitude of the T-wave in large magnetic fields has been attributed to the superposition of an induced potential associated with pulsatile blood flow into the aortic vessel.[16-19] For a rat with an average cardiac output of 47 cm^3/min and an ascending aortic diameter of 2.6 mm, the maximum induced potential within the aorta in a 1.0 T field would be predicted from eqn. (8) to be 0.4 mV. For an adult human with an average cardiac output of 5100 cm^3/min and an aortic diameter of 1.6 cm, the maximum induced aortic flow potential in a 1.0 T field is 6.8 mV. This calculation suggests that the magnitude of magnetically-induced blood flow potentials should be greater for large relative to small animal species, and

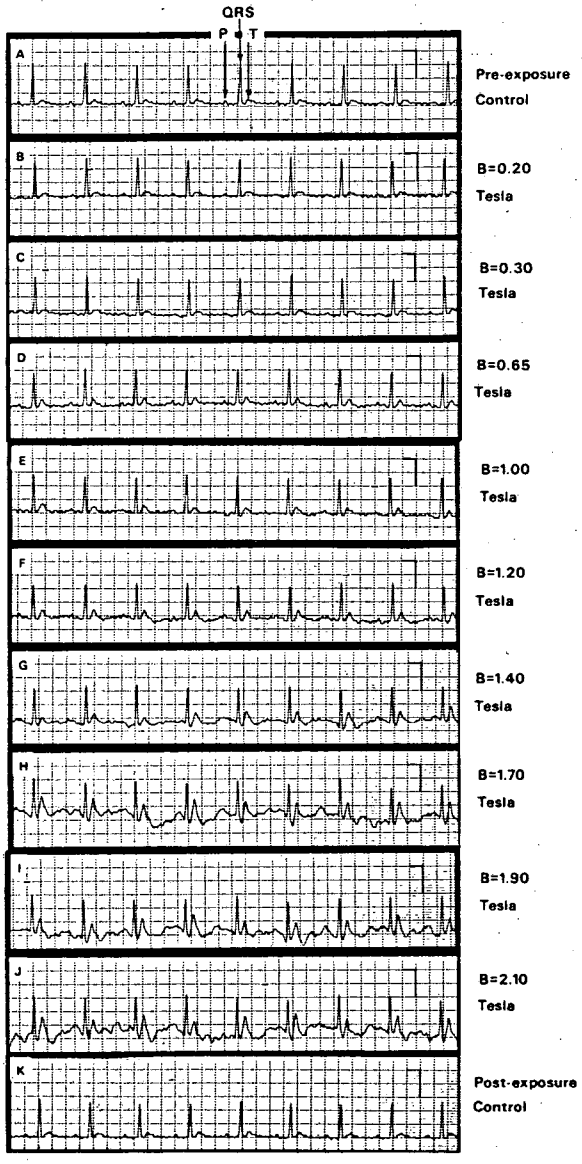

Fig. 1. Electrocardiogram records of an adult male rat are shown prior to magnetic field exposure (A), during the application of fields ranging from 0.20 to 2.10 Tesla (B to J), and immediately following magnetic field exposure (K). An increase in signal amplitude at the locus of the T wave is evident at field levels above 0.30 Tesla. The horizontal and vertical calibration bars on the ECG records represent 40 ms and 500 μV, respectively. [From C.T. Gaffey and T.S. Tenforde, Bioelectromagnetics 2:357 (1981). Reproduced with permission of the authors and publisher (Alan R. Liss, Inc.).]

experimental data related to this point will be presented in the following chapter.[20]

The interaction of an applied magnetic field with a flowing electrolyte solution will also create a net volume force equal to $\vec{J} \times \vec{B}$, where $\vec{J} = -\sigma(\vec{v} \times \vec{B})$ is the ionic conduction current resulting from the induced electric field and σ is the electrical conductivity of the medium. This interaction leads to a magnetohydrodynamic effect in which the axial flow velocity of the fluid is retarded in the presence of a stationary magnetic field. The magnitude of this effect can be estimated for the case of blood flow by solving the Navier-Stokes equation for steady laminar fluid flow in a rigid cylindrical vessel:[21,22]

$$\rho \frac{\partial \vec{v}}{\partial t} = -\nabla P + \eta \nabla^2 \vec{v} + \vec{J} \times \vec{B} \qquad (9)$$

where ρ = solution density, ∇P = pressure gradient, and η = kinematic viscosity. Eqn. (9) relates the net inertial force within the fluid to the algebraic sum of the pressure gradient that drives the flow and the viscous force and magnetic volume force that retard it. Solving eqn. (9) for a cylindrical vessel of radius R, and applying boundary conditions appropriate to the laminar flow of a viscous imcompressible fluid, gives the following expression for the axial flow velocity:

$$v = -\frac{R^2}{\eta H_a^{\,2}} \left(\frac{dP}{dz}\right) \frac{I_o(H_a) - I_o(H_a r/R)}{I_o(H_a)} \qquad (10)$$

In eqn. (10), I_o is the modified Bessel function of zero order and H_a is the Hartmann number defined as:[23]

$$H_a = BR\,(\sigma/\eta)^{\frac{1}{2}} \qquad (11)$$

The strength of the magnetohydrodynamic interaction is reflected by the magnitude of the Hartmann number. For values of $H_a \ll 1$ the magnetic interaction with ionic conduction currents is weak, and eqn. (10) reduces to the usual parabolic relation between v and the radial coordinate r. For the specific case of human blood with $\sigma = 0.519$ S/m and $\eta = 4.65 \times 10^{-3}$ kg/m•s,[19] $H_a = 0.106$ B (with B in Tesla) for flow in an aortic vessel with R = 0.01 m. The value of H_a is therefore significantly less than unity at the field levels to which humans are generally exposed. Under the condition $H_a \ll 1$, an expansion of the modified Bessel functions in eqn. (10) to second order terms gives the approximate relationship:

$$v(B) \simeq -\frac{R^2}{4\eta}\left(\frac{dP}{dz}\right)[1-(r^2/R^2)][1-(H_a{}^2/4)]$$

$$= v(B=0)[1-(H_a{}^2/4)] \qquad (12)$$

At a field intensity of 2.0 T, eqn. (12) predicts that the mean axial flow velocity in the human aorta is reduced by only 1.1% as a result of the magnetohydrodynamic interaction. Experimental data on the dynamic properties of blood flow in fields of this magnitude will be presented in the following chapter.[20]

Another biological process involving ionic flows that are subject to electrodynamic interaction with an applied magnetic field is the conduction of electrical impulses in nerve tissue. Wikswo and Barach[24] have calculated the magnetic field strength that could produce a deflecting force on nerve ionic currents equal to one tenth the force they experience from interaction with the electric field of the nerve membrane. From the Lorentz force law (eqn. 7), a magnetic interaction of this strength would require a magnetic field $B = 0.1\ E/v$, where v is the velocity of the ion currents and E is the membrane field. Since $E = \rho nqv$, where ρ = resistivity and n = density of ionic charge carriers, it follows that $B = 0.1\ \rho nq$. Assigning values of $\rho = 0.5\ \Omega\cdot m$ and $nq = 480\ C/m^3$, which are at the lower limit of the actual values expected for membrane ionic flows, then B = 24 T to produce a perturbing magnetic force that is one tenth as strong as the membrane electrical force. This simple theoretical model suggests that fields with intensities of 2.0 T or less should not produce a measurable change in the conduction velocity of nerve impulses, and this conclusion is supported by experimental data such as that shown in Fig. 2.

Theoretical analyses of magnetic field interactions with nerve ionic currents have also been made by Liboff[25] and Valentinuzzi.[26] Liboff has raised the interesting question of whether time variations in the magnetic flux linkage with ion current loops along the nerve membrane could lead to significant induced potentials. Due to the rotational symmetry of the nerve axon, it is expected that these induced electrical fields would cancel. However, for the unlikely condition of highly asymmetric current loops, Liboff[25] concluded that applied fields of less than 1.0 T could theoretically introduce significant perturbations in the membrane current flows during impulse conduction.

Magnetomechanical Effects

1. Orientation of diamagnetically anisotropic macromolecules. A large number of diamagnetic biological macromolecules exhibit orientation in strong magnetic fields. In general, these macro-

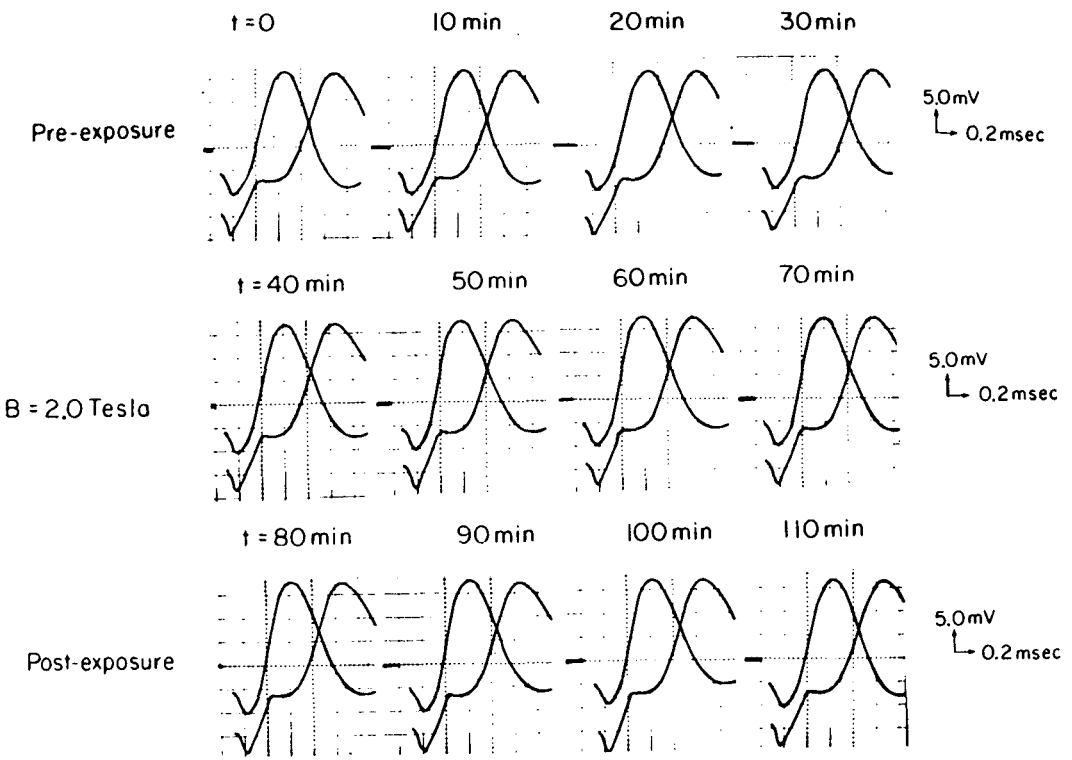

Fig. 2. Measurements of the conduction velocity of an evoked action potential along a frog sciatic nerve are shown before, during and after exposure to a 2.0-Tesla field. Each action potential was recorded at two points separated by a distance of 1.0 cm along the nerve axis. [From C.T. Gaffey and T.S. Tenforde, Radiat. Environ. Biophys. 22:61 (1983). Reproduced with permission of the authors and publisher (Springer-Verlag).]

molecules have a rodlike shape, and magneto-orientation occurs as the result of an anisotropy in the magnetic susceptibility tensor, $\bar{\bar{\chi}}$, along the different axes of symmetry. The magnetic moment per unit volume, $\vec{M}$, of these molecules in a field with intensity $\vec{H}$ is equal to $\bar{\bar{\chi}}\cdot\vec{H}$. The interaction energy per unit volume is $-\vec{B}\cdot\vec{M}\simeq-\mu_0\vec{H}\cdot\vec{M}$, and the total energy, U, is obtained by integration over the molecular volume:[27]

$$U = -\tfrac{1}{2}\iiint \vec{B}\cdot\bar{\bar{\chi}}\cdot\vec{H}dV$$

$$= -\tfrac{1}{2}\mu_0 VH^2[\chi_z + (\chi_z - \chi_r)\cos^2\theta] \qquad (13)$$

where V is the molecular volume, χ_z and χ_r are the magnetic susceptibilities along the axial (z) and radial (r) coordinates of the rod, and θ is the angle between the direction of the field and the z axis. This relationship holds for both paramagnetic and diamagnetic substances. Based on the fact that the rodlike molecules will rotate to achieve a minimum energy, then the equilibrium orientation will be at $\theta = 0$ or π if $\chi_z > \chi_r > 0$ (paramagnetic) or $\chi_r < \chi_z < 0$ (diamagnetic). The equilibrium orientiation will be at $\theta = \pi/2$ if $\chi_r > \chi_z > 0$ (paramagnetic) or $\chi_z < \chi_r < 0$ (diamagnetic).

For individual macromolecules, the magnetic interaction energy predicted by eqn. (13) will be small compared to the thermal interaction energy, kT, unless enormous field strengths are used. This fact has been demonstrated for DNA solutions in which the extent of magneto-orientation has been studied from measurements of magnetically-induced birefringence (the Cotton-Mouton effect). The probability of molecular alignment in a parallel ($P_\parallel$) as opposed to a perpendicular ($P_\perp$) configuration relative to the magnetic field direction is given by the Boltzmann relation:

$$\frac{P_\parallel - P_\perp}{P_\perp} = e^{-\Delta U/kT} - 1 \sim \mu_0 VH^2(\chi_\parallel - \chi_\perp)/kT \qquad (14)$$

In eqn. (14) it is assumed that $\Delta U/kT \ll 1$, appropriate to weak interactions between the macromolecule and the applied magnetic field. The refractive index difference, Δn, determined by optical birefringence measurements along parallel and perpendicular axes relative to the magnetic field lines will therefore depend on the square of the magnetic field intensity. The dependence of Δn on H^2 has been confirmed in birefringence measurements on calf thymus DNA,[28,29] for which the degree of orientation as defined in eqn. (14) reaches a level of only 1% in a applied field of 13 T.

Despite the weak interaction of individual macromolecules

with intense magnetic fields, there are several examples of macromolecular assemblies which exhibit orientation in fields of 1 T or less. This phenomenon results from a summation of the diamagnetic anisotropies of the individual molecules within the assembly, thereby giving rise to a large effective anisotropy and magnetic interaction energy for the entire molecular aggregate. Examples of biological systems that exhibit orientation in fields of 1 T or less are retinal rod outer segments,[30-36] photosynthetic systems (chloroplast grana, photosynthetic bacteria and Chlorella cells),[37-41] purple membranes of Halobacteria[42] and muscle fibers.[43] Several of the physical principles underlying magneto-orientation phenomena have been experimentally demonstrated for retinal rod outer segments, and the following discussion will therefore be focused on this specific system.

The first observation that isolated rod outer segments, which consist of pigmented disk membranes stacked in a regular array, will orient in a 1 T stationary magnetic field was made in 1970.[30] The oriented segments are aligned with the disk membranes perpendicular to the applied field direction, which indicates that magneto-orientation results from the large summed diamagnetic anisotropy of the rhodopsin photopigments, as opposed to the lamellar membrane phospholipids.[31,34] An estimate of the summed anisotropy, $V(\chi_z - \chi_r)$, for the rod outer segments can be obtained by observing the kinetics of the magneto-orientation process. If the rods are modeled as cylinders of diameter d and length L, then the equation of motion in a magnetic field oriented at an angle θ relative to the long axis of the rod is given by

$$\frac{I}{2}\frac{d^2\theta}{dt^2} + \xi\frac{d\theta}{dt} + \frac{\partial U}{\partial\theta} = 0 \qquad (15)$$

where I is the moment of inertia of the rods and ξ the frictional coefficient:

$$\xi \simeq \frac{2\pi\eta L^3/3}{2\ln(2L/d)-1} \qquad (16)$$

The third term on the left hand side of eqn. (15) is the magnetic orientational force, which can be calculated from eqn. (13):

$$\partial U/\partial\theta = [\mu_0 V H^2(\chi_z-\chi_r)\sin 2\theta]/2 \qquad (17)$$

The inertial term in eqn. (15), $(I/2)d^2\theta/dt^2$, is small and can be neglected relative to the frictional resistance, $\xi d\theta/dt$, and the magnetic force, $\partial U/\partial\theta$. Accordingly, eqn. (15) can be directly integrated to give:

$$t = \frac{-2\xi}{\mu_0 V H^2(\chi_z - \chi_r)} \int_{\theta_o}^{\theta_1} \csc 2\theta \, d\theta \qquad (18)$$

which becomes

$$\ln \tan\theta_1 = \ln \tan\theta_o - \frac{\mu_0 V H^2(\chi_z - \chi_r)t}{\xi} \qquad (19)$$

The time for rods to rotate through $\pi/2$ radians is predicted from eqn. (19) to be approximately 4 s in a 1.0 T field, and this number agrees well with experimental observations on the kinetics of rod orientation.[32] The kinetic relation given in eqn. (19) also provides a method for calculating the summed diamagnetic anisotropy, since a plot of $\ln \tan \theta$ versus time will have a slope proportional to $V(\chi_z - \chi_r)$. By this method Hong[35] has estimated the summed anisotropy of rod outer segments from the frog to be 9 x 10^{-4} e.m.u./mol.

2. Orientation of organisms with permanent magnetic moments. A fascinating specimen for the biophysical study of magnetic field interactions was provided by Blakemore's accidental discovery of magnetotactic bacteria.[44] Approximately 2% of the dry mass of these aquatic organisms is iron, which has been shown by Mössbauer spectroscopy to be predominantly in the form of magnetite: Fe_3O_4.[45] The magnetite crystals are arranged as chains of approximately 20-30 single domain cyrstals, as shown in Fig. 3. The orientation of the net magnetic moment is such that magnetotactic bacteria in the northern hemisphere migrate towards the north pole of the geomagnetic field, whereas strains of these bacteria that grow in the southern hemisphere move towards the south magnetic pole.[46] Magnetotactic bacteria that have been found at the geomagnetic equator are nearly equal mixtures of south-seeking and north-seeking organisms.[47] Because of the polarities of their magnetic moments, the magnetotactic bacteria in both the northern and southern hemispheres migrate downwards in response to the vertical component of the geomagnetic field. It has been proposed that this downward directed motion, which carries the bacteria into the bottom sediments of their aquatic environment, may be essential for the survival of these microaerophilic organisms.[44,45]

The magnetotactic bacterium swims by flagellar propulsion, and the mean rate of migration is a function of the average cosine of the angle θ between the magnetic moment of the bacterium and the geomagnetic field.[10] The interaction energy, U, of the bacterial magnetic moment, $\vec{m}$, and the field, $\vec{B}$, is $U = -\vec{m}\cdot\vec{B} = -mB\cos\theta$. From Boltzmann statistics, the average value of $\cos \theta$ is given by:

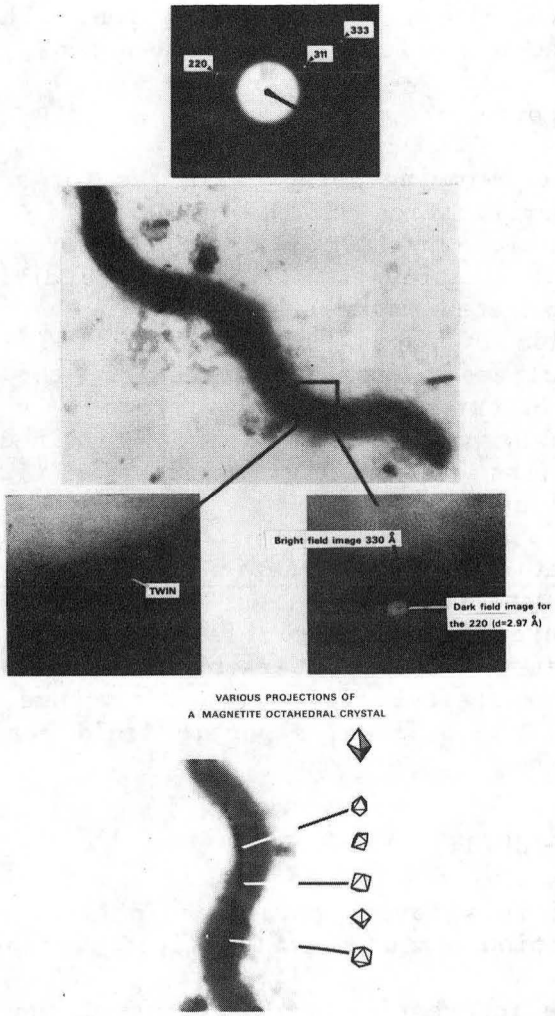

XBB 8311-10041

Fig. 3. Electron micrographs of a fresh water magnetotactic bacterium. The dark field image at the right corresponds to the indicated bright field image of a magnetite crystal. The majority of the crystals are single domain magnetite octahedra. [Courtesy of Dr. Thomas F. Budinger, University of California, Berkeley.]

$$\langle\cos\theta\rangle = \frac{\int_0^\pi \cos\theta e^{-U/kT} d\theta}{\int_0^\pi \ell^{-U/kT} d\theta}$$

$$= \coth(mB/kT)-(mB/kT)^{-1} \qquad (20)$$

which is the well-known Langevin function. The mean rate of migration of the bacterium, $\langle v\rangle$, is given by

$$\langle v\rangle = v_o\langle\cos\theta\rangle \qquad (21)$$

where v_o is the swimming velocity in the forward direction. An experimental verification of the relationship between $\langle v\rangle$ and $\langle\cos\theta\rangle$ has been made by Kalmijn,[10] who measured $\langle v\rangle$ as a function of magnetic field strength for several individual bacteria contained in isolated water droplets. In the 50 μT geomagnetic field, the value of $\langle\cos\theta\rangle$ ranged from 0.80 - 0.88 for the individual specimens. From these results, the average magnetic moment of the bacteria was estimated to be 7×10^{-16} J/T, which agrees reasonably well with values determined by physical techniques such as elastic light scattering[48] and magnetically-induced birefringence.[49]

3. Translation of paramagnetic substances in a magnetic field gradient. A material with a net magnetic moment, $\vec{m}$, will experience a force in a magnetic field gradient that is given by $-\nabla U = \nabla\vec{m}\cdot\vec{B}$, where U is the interaction energy. If the substance has a magnetic susceptibility, χ, and a volume, V, the magnetic moment $\vec{m} = \chi V\vec{H}$. In a linear magnetic field gradient, dH/dz, the force is given by

$$F(z) = \frac{\chi VH}{\mu_o}(dH/dz) \qquad (22)$$

As a result of this force, paramagnetic materials will migrate along the direction of the magnetic field gradient.

One of the interesting applications of the magnetomechanical force exerted by a magnetic field gradient is the differential separation of erythrocytes from whole blood.[50,51] In this procedure a magnetic field of approximately 2 T is used to magnetize a stainless steel wire mesh packed within a polyethylene cylinder, thereby creating local field gradients approaching 10^4 T/m near the wires. Blood is applied to the column after dilution in an isotonic solution that contains sodium dithionite to reduce the erythrocyte hemoglobin to its paramagnetic deoxyhemoglobin form. When the column is flushed with buffer solution while the magnetic field is being applied, elution of the nonerythroid blood cells occurs while the erythrocytes are retained on the magnetized

wire mesh. The field is then switched off and the column is again flushed with buffer solution, producing a pure erythrocyte cell population in the eluant. Up to 70% of the total erythrocyte population can be retained in the column while the field is being applied, thereby producing a significant enrichment of the nonerythroid cell populations such as white blood cells and platelets.

Magnetic Field Interactions at the Atomic and Nuclear Levels

1. Nuclear magnetic resonance. During the last decade rapid progress has been made in using nuclear magnetic resonance (NMR) to obtain high-resolution images of biological tissues.[52-56] In this technique, nuclear magnetic moments are aligned by the application of a stationary magnetic field, H_o, and undergo a precessional motion about the field direction with a characteristic frequency $\nu = \gamma H_o/2\pi$. The constant γ is the gyromagnetic ratio, defined as the nuclear magnetic moment divided by the spin angular momentum. When a radiofrequency field is applied transverse to the direction of H_o, it can undergo a resonant interaction with the aligned magnetic moments that cause them to adopt the antiparallel state. As the nuclear moments return to their equilibrium state, they radiate a quantum of energy that is proportional to the resonant frequency. The overall strength of the radiated signal picked up in a receiver coil reflects the total tissue concentration of magnetic nuclei such as protons. In addition, the time variation in the decay of the NMR signal provides a rich variety of information about the local environment of the magnetic nuclei. These time parameters include the spin-lattice relaxation time T_1, which conveys information on the regional temperature and viscosity, and the spin-spin relaxation time T_2, which reflects the local magnetic field resulting from the nuclear moments of neighboring nuclei. The T_1 and T_2 parameters provide information that can be converted into contrast differences in NMR images of tissue proton density. In proton-rich structures such as myelinated nerves in the central nervous system, regions of demyelination can be sharply defined by NMR images based on the T_1 or T_2 relaxation parameters. The development of demyelination disorders such as multiple sclerosis may therefore be detected with a greater sensitivity using NMR imaging than other contemporary imaging modalities. Proton magnetic resonance also shows promise as an effective imaging modality for the detection of malignancies.

In addition to its use as a noninvasive imaging modality, NMR spectroscopy based on ^{31}P signals has been shown to provide detailed information on the dynamics of tissue metabolism.[57,58] The ^{31}P signals provide a direct measure of the relative concentrations of ATP, phosphocreatine and inorganic phosphates during oxidative phosphorylation processes in organs such as the heart.

2. Charge transfer reactions. A number of organic reaction processes that involve electron transfer via radical pair intermediates are highly sensitive to magnetic field interactions. A well-studied example that is biologically relevant is the photoinduced charge transfer reaction that occurs in bacterial photosynthesis.[59-64] Within 10 ps following excitation of bacteriochlorophyll $(BCh\ell)_2$ to its first excited singlet state, a radical pair intermediate state is formed that consists of a $(BCh\ell)_2^{+}\cdot$ cationic dimer and a bacteriopheophytin $(BPh)^{-}\cdot$ anion. Within 200 ps electron transfer occurs to the ultimate acceptor, a ubiquinone-iron complex. However, if the acceptor molecule is chemically reduced, the lifetime of the radical pair intermediate state increases to approximately 10 ns. With an extended lifetime, hyperfine interactions between the nuclear and electron spin magnetic moments leads to an interconversion of the radical pairs between the singlet and triplet states. Under this condition, the intermediate state decays directly back to the singlet ground state, or decays via a metastable triplet state. Because of the weakness of the hyperfine interaction, the triplet states are nearly degenerate and the electron spins of the radical pair intermediate can move with nearly equal probabilities between the singlet S_o and the triplet T_o and $T_{\pm 1}$ states. However, in the presence of an applied magnetic field that exceeds approximately 1 mT, the resulting Zeeman interaction with the radical electron spins will lift the degeneracy of the triplet state and effectively block the $T_{\pm 1}$ triplet channels. Theoretically, the yield of triplet product should be reduced by two thirds in the presence of the external field, and this has been confirmed experimentally by laser pulse excitation and optical absorption measurements.[62] Because of the relatively low field strengths that influence the radical pair intermediate states in the charge transfer process, this phenomenon may have interesting implications for similar chemical reaction processes in other biological systems. However, it must be emphasized that the model photosynthetic systems studied to date have been artificially placed in an abnormal state by chemical reduction of the ultimate electron acceptor molecules.

TIME-VARYING MAGNETIC FIELDS

In accord with Faraday's law, magnetic fields that vary in time will induce potentials and circulating currents in biological tissues. To illustrate the relevant physical principles, a calculation will be made of the peak field and current density induced in a circular loop of radius r during exposure to a sinusoidal magnetic field $\vec{B} = \vec{B}_o \sin 2\pi\nu t$, where ν is the frequency. The magnitude of the peak induced potential ψ_{peak} around the loop is given by Faraday's law:

$$\psi_{peak} = \left| \frac{d(\vec{B}\cdot\vec{S})}{dt} \right|_{peak} = 2\pi^2 r^2 \nu \, |\vec{B}_o| \tag{23}$$

In eqn. (22) the peak potential is calculated for the condition that the field is normal to the plane of the loop, and hence parallel to its area vector, $\vec{S}$. The peak induced electric field $|\vec{E}|_{peak}$ is given by

$$|\vec{E}|_{peak} = \frac{\psi_{peak}}{2\pi r} = \pi r \nu \, |\vec{B}_o| \tag{24}$$

and the peak current density $|\vec{J}|_{peak}$ by

$$|\vec{J}|_{peak} = \sigma |\vec{E}|_{peak} = \pi r \nu \sigma \, |\vec{B}_o| \tag{25}$$

where σ is the electrical conductivity. One aspect of eqns. (24) and (25) is the dependence of the induced field and current on the radius of the loop through which magnetic flux linkage occurs. An important implication of this result for biological systems is that time-varying fields of modest strength (1 mT or less) may induce significant circulating currents at the macroscopic level, but substantially smaller induced currents will be produced at the cellular level.

A well-documented biological effect of time-varying magnetic fields is the occurrence of magnetophosphenes, which were first observed by d'Arsonval in 1896.[65] In this phenomenon, the sensation of flickering light is induced when the eye is exposed to magnetic fields with flux densities greater than 10 mT and frequencies greater than 10 Hz. The minimum field strength required to produce visual phosphenes occurs at a frequency of 20 Hz.[66-69] By using a microelectrode technique to record electrical signals from retinal ganglion cells, it has been demonstrated that 20 Hz fields with flux densities above the phosphene threshold level act to increase by 4 ms the latency interval between the administration of a light stimulus and the response of the ganglion cells.[70] When the continuity of the visual response pathway between the photoreceptors and the retinal ganglion cells was blocked by addition of cobalt chloride or sodium aspartate to an <u>in vitro</u> frog eye preparation, the electrical response of the ganglion cells to an oscillating magnetic field disappeared.[70] This observation suggests that the locus of the time-varying magnetic field effect is in the photoreceptors rather than in the post-synaptic neurons.

Another potentially important target of ELF magnetic field

interactions is the nervous system. From a consideration of the naturally occurring fields in the central nervous system, Bernhardt[71] concluded that magnetic fields in the 1-100 Hz frequency range would have to induce current densities in tissue of approximately 1 mA/m^2 or larger to have a direct effect on the brain's electrical activity. The strength of a 60-Hz magnetic field that would induce a peak current density of this magnitude in the cranium of a human subject can be calculated in an approximate manner from eqn. (25). Assuming the conductivity, σ, to have an average value of 0.1 S/m,[71] and setting r = 0.1 m, then $|\vec{B}_o| = 0.53$ mT to induce a peak current density of 1 mA/m^2 in the peripheral region of the cranium. In a careful study of human preception to 60-Hz magnetic fields, Tucker and Schmitt[72] found no significantly perceptive individuals among more than 200 subjects exposed to a 1.5 mT (rms) [$|\vec{B}_o| = 2.1$ mT] field. Several behavioral tests with mice exposed to 60-Hz magnetic fields that induce peak current densities approaching 1 mA/m^2 in the peripheral cranial region have also yielded negative findings.[73] The results of these studies suggest that ELF magnetic fields must have significantly greater amplitudes than the theoretically calculated threshold values in order to perturb animal behavior. It is important, however, to recognize the inherent deficiencies of a simple theoretical model that treats the central nervous system as a region of uniform conductivity. In addition, the induced current in a loop of maximum radius at the brain's surface may not be the relevant parameter to consider in predicting the response to ELF magnetic fields. The regions of the central nervous system that might be responsive to these fields may have significantly smaller dimensions than the entire cranium, thereby necessitating a large increase in the ELF magnetic field strength that would be required to evoke a measurable electrical and/or behavioral perturbation.

ACKNOWLEDGMENTS

The excellent secretarial assistance of K. Kalman is gratefully acknowledged. Magnetic field research in the author's laboratory is supported by the Office of Energy Research, Health and Environmental Research Division, of the U.S. Department of Energy under Contract No. DE-AC03-76SF00098 with the Lawrence Berkeley Laboratory.

REFERENCES

1. F. W. Cope, Evidence from activation energies for superconductive tunneling in biological systems at physiological temperatures, Physiol. Chem. Phys. 3:403 (1971).

2. E. H. Halpern and A. A. Wolf, Speculations of superconductivity in biological and organic systems, in: "Cryogenic Engineering," Vol. 17, K. D. Timmerhaus, ed., Plenum, New York (1972).
3. F. W. Cope, Biological sensitivity to weak magnetic fields due to biological superconductive Josephson junctions?, Physiol. Chem. Phys. 5:173 (1973).
4. J. P. Marton, Conjectures on superconductivity and cancer, Physiol. Chem. Phys. 5:259 (1973).
5. K. Antonowicz, Possible superconductivity at room temperature, Nature 247:358 (1974).
6. F. W. Cope, Enhancement by high electric fields of superconduction in organic and biological solids at room temperature and a role in nerve conduction?, Physiol. Chem. Phys. 6:405 (1974).
7. F. W. Cope, On the relativity and uncertainty of electromagnetic energy measurement at a superconductive boundary. Application to perception of weak magnetic fields by living systems, Physiol. Chem. Phys. 13:231 (1981).
8. A. J. Kalmijn, The detection of electric fields from inanimate and animate sources other than electric organs, in: "Handbook of Sensory Physiology," H. Autrum, R. Jung, W. R. Loewenstein, D. M. MacKay, and H. L. Teuber, eds., Springer-Verlag, New York (1974).
9. A. J. Kalmijn, Experimental evidence of geomagnetic orientation in elasmobranch fishes, in: "Animal Migration, Navigation, and Homing," K. Schmidt-Koenig and W. T. Keeton, eds., Springer-Verlag, New York (1978).
10. A. J. Kalmijn, Biophysics of geomagnetic field detection, IEEE Trans. Mag. MAG-17:1113 (1981).
11. A. Kalmijn, Electric and magnetic field detection in elasmobranch fishes, Science 218:916 (1982).
12. A. Kolin, An alternating field induction flow meter of high sensitivity, Rev. Sci. Instrum. 16:109 (1945).
13. A. Kolin, Improved apparatus and technique for electromagnetic determination of blood flow, Rev. Sci. Instrum. 23:235 (1952).
14. C. J. Mills, The electromagnetic flowmeter, Med. Instrum. 11:136 (1977).
15. D. E. Beischer and J. C. Knepton, Influence of strong magnetic fields on the electrocardiogram of squirrel monkeys (Saimiri sciureus), Aerosp. Med. 35:939 (1964).
16. T. Togawa, O. Okai, and M. Oshima, Observation of blood flow E.M.F. in externally applied strong magnetic fields by surface electrodes, Med. Biol. Engin. 5:169 (1967).

17. D. E. Beischer, Vectorcardiogram and aortic blood flow of squirrel monkeys (Saimiri sciureus) in a strong superconductive electromagnet, in: "Biological Effects of Magnetic Fields," M. Barnothy, ed., Plenum, New York (1969).
18. C. T. Gaffey and T. S. Tenforde, Alterations in the rat electrocardiogram induced by stationary magnetic fields, Bioelectromagnetics 2:357 (1981).
19. T. S. Tenforde, C. T. Gaffey, B. R. Moyer, and T. F. Budinger, Cardiovascular alterations in Macaca monkeys exposed to stationary magnetic fields: experimental observations and theoretical analysis, Bioelectromagnetics 4:1 (1983).
20. T. S. Tenforde, Biological effects of strong magnetic fields, in: "Biological effects and dosimetry of non-ionizing radiation: static and ELF electromagnetic fields," M. Grandolfo, S. M. Michaelson, and A. Rindi, eds., Plenum, New York (1984).
21. V. A. Vardanyan, Effect of a magnetic field on blood flow, Biofiz. 18:491 (1973).
22. V. M. Abashin and G. I. Yevtushenko, Concerning the paper by V. A. Vardanyan "Effect of the magnetic field on the flow of blood" printed in "Biofizika" 18:No. 3, 515, 1973, Biofiz. 19:1107 (1974).
23. J. Hartmann, Hg-dynamics I: Theory of the laminar flow of an electrically conductive liquid in a homogeneous magnetic field, Klg. Danske Videnskab. Selskab. Math.-fys. Medd. 15(6):1 (1937).
24. J. P. Wikswo, Jr. and J. P. Barach, An estimate of the steady magnetic field strength required to influence nerve conduction, IEEE Trans. Biomed. Engin. BME-27:722 (1980).
25. R. L. Liboff, Neuromagnetic thresholds, J. Theor. Biol. 83:427 (1980).
26. M. Valentinuzzi, Notes on magnetic actions upon the nervous system, Bull. Math. Biophys. 27:203 (1965).
27. R. B. Frankel, Biological effects of static magnetic fields, in: "Handbook of biological effects of electromagnetic fields," C. Polk and E. Postow, eds., C.R.C. Press, Boca Raton (1984).
28. G. Maret, M. v. Schickfus, A. Mayer, and K. Dransfeld, Orientation of nucleic acids in high magnetic fields, Phys. Rev. Lett. 35:397 (1975).
29. G. Maret and K. Dransfeld, Macromolecules and membranes in high magnetic fields, Physica 86-88B:1077 (1977).
30. N. Chalazonitis, R. Chagneux, and A. Arvanitaki, Rotation des segments externes des photorecépteurs dans le champ magnétique constant, C. R. Acad. Sci. Paris Ser. D 271:130 (1970).

31. F. T. Hong, D. Mauzerall, and A. Mauro, Magnetic anisotropy and the orientation of retinal rods in a homogeneous magnetic field, Proc. Natl. Acad. Sci. (USA) 68:1283 (1971).
32. R. Chagneux and N. Chalazonitis, Evaluation de l'anisotropie magnétique des cellules multimembranaires dans un champ magnétique constant (segments externes des bâtonnets de la rétine de grenouille). C. R. Acad. Sci. Paris Ser. D 274:317 (1972).
33. R. Chagneux, H. Chagneux, and N. Chalazonitis, Decrease in magnetic anisotropy of external segments of the retinal rods after a total photolysis, Biophys. J. 18:125 (1977).
34. J. F. Becker, F. Trentacosti, and N. E. Geacintov, A linear dichroism study of the orientation of aromatic protein residues in magnetically oriented bovine rod outer segments, Photochem. Photobiol. 27:51 (1978).
35. F. T. Hong, Magnetic anisotropy of the visual pigment rhodopsin, Biophys. J. 29:343 (1980).
36. M. M. Vilenchik, Magnetic susceptibility of rhodopsin, Biofiz. 27:31 (1982).
37. N. E. Geacintov, F. Van Nostrand, M. Pope, and J. B. Tinkel, Magnetic field effect on the chlorophyll fluorescence in Chlorella, Biochim. Biophys. Acta 226:486 (1971).
38. N. E. Geacintov, F. Van Nostrand, J. F. Becker, and J. B. Tinkel, Magnetic field induced orientation of photosynthetic systems, Biochim. Biophys. Acta 267:65 (1972).
39. J. F. Becker, N. E. Geacintov, F. Van Nostrand, and R. Van Metter, Orientation of chlorophyll in vivo. Studies with magnetic field oriented Chlorella, Biochem. Biophys. Res. Comm. 51:597 (1973).
40. J. Breton, The state of chlorophyll and carotenoid in vivo. II - A linear dichroism study of pigment orientation in photosynthetic bacteria, Biochem. Biophys. Res. Comm. 59:1011 (1974).
41. J. F. Becker, N. E. Geacintov, and C. E. Swenberg, Photovoltages in suspensions of magnetically oriented chloroplasts, Biochim. Biophys. Acta 503:545 (1978).
42. D.-Ch. Neugebauer and A. E. Blaurock, Magnetic orientation of purple membranes demonstrated by optical measurements and neutron scattering, FEBS Lett. 78:31 (1977).
43. W. Arnold, R. Steele, and H. Mueller, On the magnetic asymmetry of muscle fibers, Proc. Natl. Acad. Sci. (USA) 44:1 (1958).
44. R. Blakemore, Magnetotactic bacteria, Science 190:377 (1975).

45. R. B. Frankel, R. P. Blakemore, and R. S. Wolfe, Magnetite in freshwater magnetotactic bacteria, Science 203:1355 (1979).
46. R. P. Blakemore, R. B. Frankel, and A. J. Kalmijn, South-seeking magnetotactic bacteria in the Southern Hemisphere, Nature 286:384 (1980).
47. R. B. Frankel, R. P. Blakemore, F. F. Torres de Araujo, and D. M. S. Esquival, Magnetotactic bacteria at the geomagnetic equator, Science 212:1269 (1981).
48. C. Rosenblatt, F. F. Torres de Araujo, and R. B. Frankel, Light scattering determination of magnetic moments of magnetotactic bacteria, J. Appl. Phys. 53:2727 (1982).
49. C. Rosenblatt, F. F. Torres de Araujo, and R. B. Frankel, Birefringence determination of magnetic moments of magnetotactic bacteria, Biophys. J. 40:83 (1982).
50. D. Melville, F. Paul, and S. Roath, Direct magnetic separation of red cells from whole blood, Nature 255:706 (1975).
51. F. Paul, S. Roath, and D. Melville, Differential blood cell separation using a high gradient magnetic field, Brit. J. Haematol. 38:273 (1978).
52. P. C. Lauterbur, Image formation by induced local interactions: examples employing nuclear magnetic resonance, Nature 242:190 (1973).
53. P. C. Lauterbur, Medical imaging by nuclear magnetic resonance zeugmatography, IEEE Trans. Nucl. Sci. NS-26:2808 (1979).
54. P.G. Morris, P. Mansfield, I. L. Pykett, R. J. Ordidge, and R. E. Coupland, Human whole body line scan imaging by nuclear magnetic resonance, IEEE Trans. Nucl. Sci. NS-26:2817 (1979).
55. G. L. Brownell, T. F. Budinger, P. C. Lauterbur, and P. L. McGeer, Positron emission tomography and nuclear magnetic resonance imaging, Science 215:619 (1982).
56. A. R. Margulis, C. B. Higgins, L. Kaufman, and L. E. Crooks, eds., "Clinical Magnetic Resonance Imaging," Univ. Calif. Printing Dept., San Francisco (1983).
57. B. Chance, Y. Nakase, M. Bond, J. S. Leigh, Jr., and G. McDonald, Detection of ^{31}P nuclear magnetic resonance signals in brain by in vivo and freeze-trapped assays, Proc. Natl. Acad. Sci. (USA) 75:4925 (1978).
58. E. T. Fossel, H. E. Morgan, and J. S. Ingwall, Measurement of changes in high-energy phosphates in the cardiac cycle by using gated ^{31}P nuclear magnetic resonance, Proc. Natl. Acad. Sci. (USA) 77:3654 (1980).
59. R. E. Blankenship, T. J. Schaafsma, and W. W. Parson, Magnetic field effects on radical pair intermediates in bacterial photosynthesis, Biochim. Biophys. Acta 461:297 (1977).

60. H.-J. Werner, K. Schulten, and A. Weller, Electron transfer and spin exchange contributing to the magnetic field dependence of the primary photochemical reaction of bacterial photosynthesis, Biochim. Biophys. Acta 502:255 (1978).
61. R. Haberhorn and M. E. Michel-Beyerle, On the mechanism of magnetic field effects in bacterial photosynthesis, Biophys. J. 26:489 (1979).
62. M. E. Michel-Beyerle, H. Scheer, H. Seidlitz, D. Tempus, and R. Haberkorn, Time-resolved magnetic field effect on triplet formation in photosynthetic reaction centers of Rhodopseudomonas sphaeroides R-26, FEBS Lett. 100:9 (1979).
63. A. J. Hoff, Magnetic field effects on photosynthetic reactions, Quart. Rev. Biophys. 14:599 (1981).
64. A. Ogrodnik, H. W. Kruger, H. Orthuber, R. Haberkorn, M. E. Michel-Beyerle, and H. Scheer, Recombination dynamics in bacterial photosynthetic reaction centers, Biophys. J. 39:91 (1982).
65. M. A. d'Arsonval, Dispositifs pour la mesure des courants alternatifs à toutes frequences, C. R. Soc. Biol. (Paris) 3(100 Ser.):451 (1896).
66. H. B. Barlow, H. I. Kohn, and E. G. Walsh, Visual sensations aroused by magnetic fields, Amer. J. Physiol. 148:372 (1947).
67. P. Lövsund, P. Å. Öberg, and S. E. G. Nilsson, Influence on vision of extremely low frequency electromagnetic fields, Acta Ophth. 57:812 (1979).
68. P. Lövsund, P. Å. Öberg, S. E. G. Nilsson, and T. Reuter, Magnetophosphenes: a quantitative analysis of thresholds, Med. Biol. Engin. Comput. 18:326 (1980).
69. P. Lövsund, P. Å. Öberg, and S. E. G. Nilsson, Magneto- and electrophosphenes: a comparative study, Med. Biol. Engin. Comput. 18:758 (1980).
70. P. Lövsund, S. E. G. Nilsson, and P. Å. Öberg, Influence on frog retina of alternating magnetic fields with special reference to ganglion cell activity, Med. Biol. Eng. Comput. 19:679 (1981).
71. J. Bernhardt, The direct influence of electromagnetic fields on nerve and muscle cells of man within the frequency range of 1 Hz to 30 MHz, Radiat. Envir. Biophys. 16:309 (1979).
72. R. D. Tucker and O. H. Schmitt, Tests for human perception of 60 Hz moderate strength magnetic fields, IEEE Trans. Biomed. Eng. BME-25:509 (1978).
73. H. P. Davis, S. J. Y. Mizumori, H. Allen, M. R. Rosenzweig, E. L. Bennett, and T. S. Tenforde, Behavioral studies with mice exposed to DC and 60-Hz magnetic fields, Bioelectromagnetics 5:147 (1984).

This report was done with support from the Department of Energy. Any conclusions or opinions expressed in this report represent solely those of the author(s) and not necessarily those of The Regents of the University of California, the Lawrence Berkeley Laboratory or the Department of Energy.

Reference to a company or product name does not imply approval or recommendation of the product by the University of California or the U.S. Department of Energy to the exclusion of others that may be suitable.

TECHNICAL INFORMATION DEPARTMENT
LAWRENCE BERKELEY LABORATORY
UNIVERSITY OF CALIFORNIA
BERKELEY, CALIFORNIA 94720